# Structural Health Monitoring of Urban Infrastructures with Time-Series InSAR Analysis

*Xiaoqiong QIN*[a], *Mingsheng LIAO*[a,b], *Mengshi YANG*[a]

[a] State Key Laboratory of Information Engineering in Surveying Mapping and Remote Sensing, Wuhan University, Wuhan 430079, China

[b] Collaborative Innovation Center for Geospatial Technology, Wuhan, China

## ABSTRACT

The intensive urban infrastructures including roads, subways and high-speed railways are closely related to the sustainable economic development and social stability, and also supporting spatial distribution of various functions within the city. To ensure the security and sustainable development of transportation, we evaluated the potential of high resolution time-series Interferometric Synthetic Aperture Radar (InSAR) technology in monitoring the deformations of different types of infrastructures. A spatial-temporal strategy effectively combines SAR amplitude, interferometric phase and a priori information of structures to maximize the point-like targets (PTs). High density of PTs was identified and facilitated analyzing the deformation character of individual structures. Taking Shanghai, a coastal city with severe land subsidence, as an example, the detail spatial and temporal varying patterns and possible driven force of the deformations of typical transportation infrastructures were revealed. The accuracy of our results was verified by leveling data in the same period and showed fairly consistent agreement. This study further illustrated that it is feasible to use the high resolution time-series Interferometric Synthetic Aperture Radar (InSAR) technology into the structural health monitoring and early warning of urban infrastructures.

***Index Terms*** — Urban infrastructures, InSAR, structural health, time-series, Shanghai

## 1. INTRODUCTION

With the rapid development of population and economy in populated cities, the transport infrastructure is accelerated aging [1]-[2]. Shanghai, a coastal city in eastern China, experienced severe land subsidence since the last century [3]-[4]. Over the past decade, Shanghai has made an enormous effort in expanding its transportation infrastructures and related facilities. Shortage of timely effective deformation monitoring may lead to major accidents if the accumulation deformation is beyond the prescribed limits. Consequently, the periodically monitoring of land subsidence caused by natural processes or anthropogenic activities along the infrastructures is extremely essential to make sure the security of human lives and sustainable development of transportation.

For many years, the structural health monitoring of urban infrastructures relied on conventional on-structure measurements conducted annually or after potential damage incidents. Given these limitations, monitoring such linear infrastructures at a large scale requires new kinds of enabling technologies, especially since deformation along these infrastructures can vary sharply both spatially and temporally [5]. Looking at the current Earth Observation science, InSAR technique has been recognized as an advanced geodetic tool, featured by the all-day and all-weather working capabilities, wide spatial coverage, fine spatial resolution and high measurement precision [6]. As manmade linear civil infrastructures usually maintain good coherence over a long time span due to its stable backscattering, PS-InSAR technology can provide a good technical support for subsidence monitoring[3]. In particular, high resolution and short wave radar data can help to improve the precision of deformation detection along linear features[7].

In this work, improvements have been made to enhance the special characteristics of the deformation monitoring along linear infrastructures. A spatial-temporal strategy effectively combines SAR amplitude, interferometric phase and a priori information of structures to maximize the point-like targets (PTs). A detailed spatial-temporal evolution of subsidence on different types of individual infrastructures was clearly identified for the purpose of risk assessment and driving force analysis. The accuracy of our results was verified by leveling data and showed fairly consistent agreement.

## 2. URBAN INFRASTRUCTURES DEFORMATION ESTIMATION

For the special characteristics of deformation monitoring on urban infrastructures, A spatial-temporal strategy effectively combines SAR amplitude, interferometric phase and a priori information of structures to maximize the point-like targets (PTs).

Since our purpose is to estimate the subsidence parameters of the transportation infrastructures, we focus our attention on identifying and analysis PTs associated with the linear structures. From the coregistered SLCs, we accurately select the stable PTs on the routes by a spatial-temporal strategy. Firstly, in temporal context, a set of points with multi-temporal amplitude stability and high backscattering intensity throughout the observation period are considered as PT candidates. As the number of images is limited, it is difficult to give a proper statistical description of points. Then, maximum likelihood of the coherence $\gamma_m$, expressed as equation (1), is used to evaluate the phase accuracy for each points, which is independent of the image number.

$$\gamma_m = \frac{1}{N}\left|\sum_{i=1}^{N} exp\{j(\delta\emptyset_{noise})\}\right| \qquad (1)$$

Where $N$ is the number of available interferograms and $\delta\emptyset_{noise}$ is the thermal noise phase. It is apparently that $\gamma_m$ is a measure of the phase stability of points and hence an indicator of whether the point is a PT [8]. In other words, we only keep the points with multi-temporal phase stability. The PT candidates are selected based on the theoretical of probabilistic distribution. A $\gamma^*$ is used to identify a maximum number of measurements points while keeping the false alarm rate below a given value $q$. The $\gamma^*$ can be calculated by

$$\frac{(1-\alpha)\int_{\gamma^*}^{1} p'(\gamma_m)d_{\gamma^*}}{\int_{\gamma^*}^{1} p(\gamma_m)d_{\gamma^*}} = q \qquad (2)$$

Where $\alpha \in [0,1]$, is the proportion of candidate being a PT. $p(\gamma_m)$ and $p'(\gamma_m)$ are the probability density function of being a PT or a random phase pixel. These two candidates based on amplitude stability and coherence are combined into one list for maximum the density of PTs [9].

Meanwhile, in spatial context, the points falling outside of the buffer zone along the routes are excluded. Phase unwrapping are then carried out on these PTs. After estimating the subsidence rates and the elevation residuals of all the PTs, a statistical analysis of the PTs in a local area of the route is carried out to get a reasonable range of elevation. If beyond the reasonable range, the PT will be identified as a false one which is not exactly on the route and be rejected.

After removing the topographic phase using a SRTM with resolution of 30m, the differential phase $\emptyset_{diff}$ on the detected PTs can be considered as the summation of four components with respect to a given reference point as below [10]:

$$\emptyset_{diff}(i) = \emptyset_{def}(i) + \emptyset_{topoerr}(i) + \emptyset_{atm}(i) + \emptyset_{noise}(i) \quad (3)$$

Where $\emptyset_{def}$ indicates the phase component related to deformation of PT $i$ in the satellite LOS direction, $\emptyset_{topoerr}$ indicates the phase component associated to the height error, $\emptyset_{atm}$ indicates the phase component due to the fluctuations of water vapor in the atmosphere and $\emptyset_{noise}$ indicates thermal noise. Then, all PTs within a given distance were connected to constitute a local network along the structures based on a balance of the computation and validity. Aiming to reduce the effect of unavoidable noise, the phase increments between neighboring PT $i$ and $j$ in an interferometric image are calculated and expressed as follows:

$$\delta\emptyset_{def}(i,j) = \delta\emptyset_{l}(i,j) + \delta\emptyset_{nl}(i,j) = \frac{4\pi}{\lambda}\cdot\Delta v\cdot B_t + \delta\emptyset_{nl}(i,j) \quad (4)$$

$$\delta\emptyset_{topoerr}(i,j) = \frac{4\pi}{\lambda}\cdot\frac{B_n}{Rsin\theta}\cdot\Delta\varepsilon \qquad (5)$$

Where $\delta\emptyset_{l}(i,j)$ and $\delta\emptyset_{nl}(i,j)$ are the linear and nonlinear component of deformation. $\Delta v$ and $\Delta\varepsilon$ are the velocity and height error increments between neighboring PTs. $B_t$ and $B_n$ are the temporal baseline and spatial normal baseline of the interferogram. λ, $R$ and $\theta$ are the wavelength, distance from satellite to target and incident angel. With a set of differential interferograms of the same area, an iterative weighted least squares adjustment is performed to estimate the topographic error and the linear deformation of all the PTs following (4) and (5). Taking into account that the atmospheric perturbation is a spatial small wavenumber signal, the neighboring atmospheric difference phase $\delta\emptyset_{atm}(i,j)$ is considered to be 0 which can be negligible.

## 3. RESULTS AND INTERPRETATIONS

To extract the deformation along the transportation infrastructures in Shanghai by the aforementioned method, we utilized 26 TerraSAR-X images from

September 2013 to October 2014. The coverages of TSX images showed in Fig.1 as the rectangles, downtown on the left and Pudong on the right.

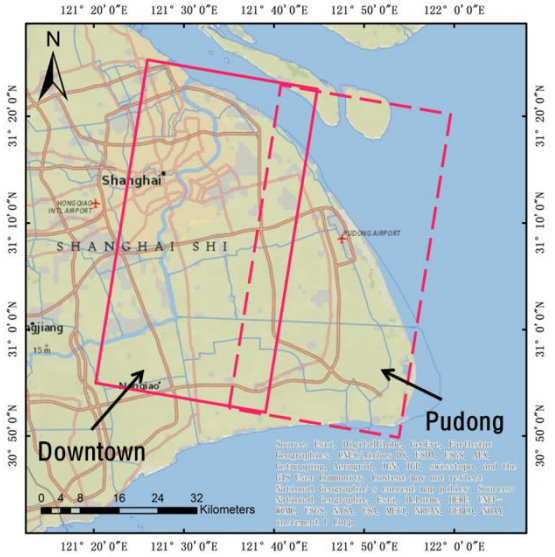


Fig.1 Coverage of the TSX images.

### 3.1. Road Networks

According to our results, the subsidence of roads network in shanghai occurs mainly in Zhangjiang and Situan area as showed in Fig.2. However, as the elevated roads usually have deeper foundation piles, they are more stable except a few sections within Zhangjiang settlement area in Fig.3.

It is apparently that the frequent urbanization construction especially the subway tunnel excavation is the main reason for the roads subsidence. Some transportation hubs, such as Longyang road and Pujiang town stations, show a lager deformation tendency in Fig.4 and Fig.5.

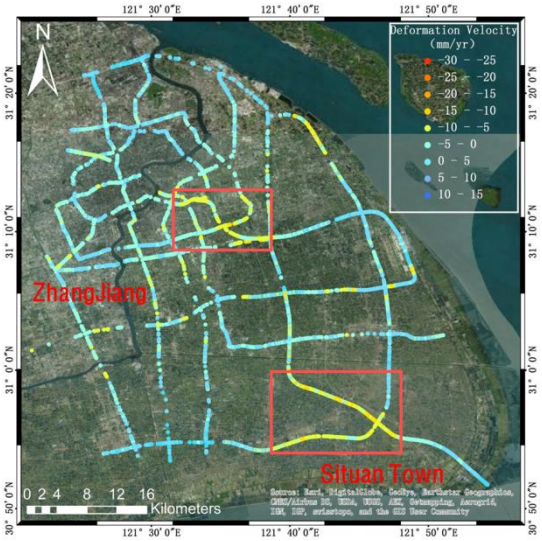


Fig.2 Deformation pattern of roads network

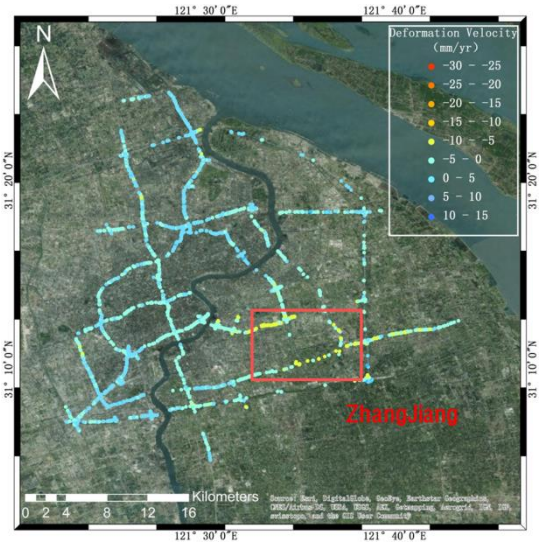


Fig.3 Deformation pattern of elevated roads

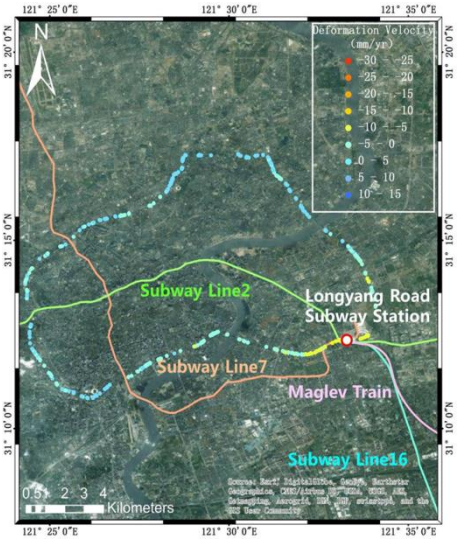


Fig.4 Deformation of Longyang Road Station


Fig.5 Deformation of Pujiang Station

## 3.2 Subway Networks

The subsidence of the subway networks in Shanghai was uneven and mainly occurred in ZhangJiang area as shewed in Fig.6.

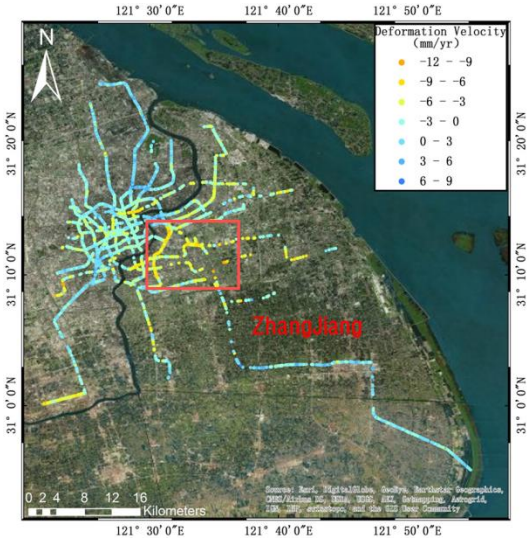


Fig.6 Deformation pattern of subway networks

From the subway with different building modes we can find various deformation characteristics in Fig.7. As elevated sections usually have deeper pile foundation, the subsidence velocities are smaller than underground sections which located in the shallow soft soil.

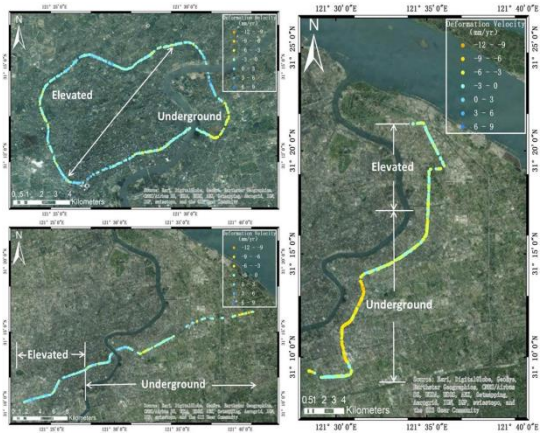


Fig.7 Deformation pattern of subway with different building modes

The subways with different construction periods also show various deformation characteristics in Fig.8. After long-term settlement and effective management and maintenance, earlier construction sections are more stable than later sections.

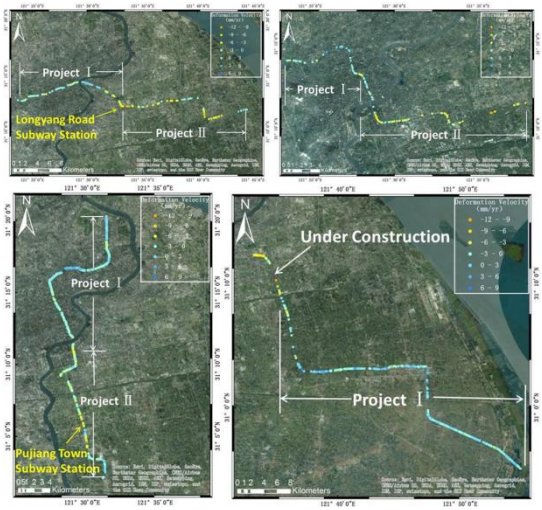


Fig.8 Deformation pattern of subway with different construction periods

## 3.3 High-speed Railways

The subsidence velocity map of the Shanghai-Hangzhou High-speed Railway from TerraSAR-X is showed in Fig.9. We can see that PTs in TerraSAR-X results can be found on the concrete or asphalt road surface. This is because some parts of the road surface can be viewed as rough targets for the short radar wavelength of 3.1 cm. The subsidence velocity is much smaller than the roads and subways. A section A near an industrial zone was identified from the mean velocity map.

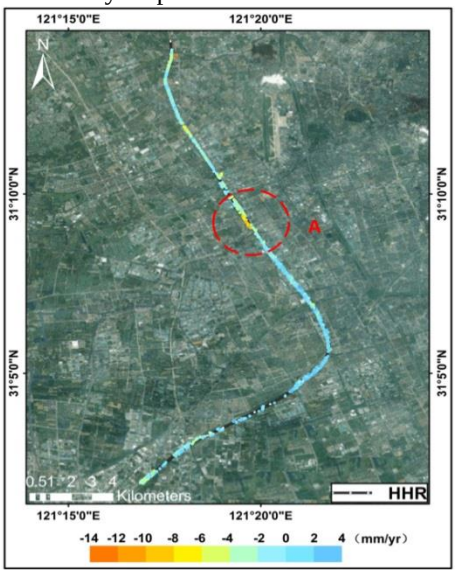


Fig.9 Deformation pattern of Shanghai-Hangzhou High-speed Railway

Shanghai Hongqiao Integrated Transportation Hub is the largest and most sophisticated integrate air-land transportation hub in the world. It integrates the civil

aviation, high-speed rail, intercity rail, maglev, metro, ground buses and taxis, creating a precedent of zero transfer between multiple transportations. The daily passenger throughput is up to 110 million people. It is therefore essential to detecting its deformation regularly. The vertical deformation patterns of Hongqiao Hub during two TerraSAR-X datasets illustrated in Fig.10 and Fig.11. Since Hongqiao hub was under construction from 2008 to 2010, very few points are selected in Fig.10 while much more points on the buildings and tracks are selected in Fig.11. It should be point out that lots of PTs are identified on the old No.1 runway but few on the new No.2 runway. From the satellite base map we can clearly find that the No.1 runway is black and the No.2 runway is white. A reasonable explanation may be they are constructed by different materials, which would indeed affect the density of PTs. The magnitude of unequal deformation caused by the expansion and operation of Hongqiao hub increased. The subsidence mainly occurs on the Shenghong mansion, No.2 terminal building and freight station of Hongqiao Airport, and the track around Hongqiao Railway Station. The runways and building of Hongqiao Railway Station remain stable. This may be related to the different requirements on the underground pile foundation and different ground loads of these structures.

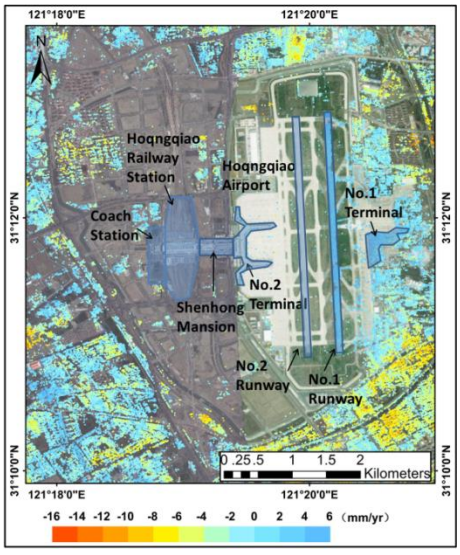


Fig.10 Deformation pattern of Hoongqiao Hub from 2008 to 2010

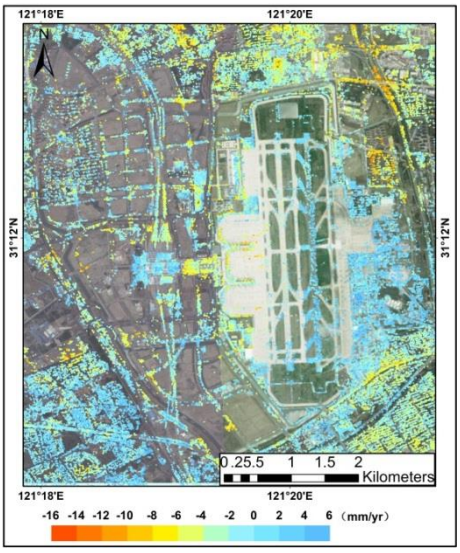


Fig.11 Deformation pattern of Hoongqiao Hub from 2010 to 2011

## 4. CONCLUSIONS AND OUTLOOKS

In this study, we investigated the potential of an improved PSI analysis approach for structural health monitoring of urban infrastructures. Our results show that the spatial-temporal strategy can be a good solution to identify a higher density of PTs along the individual tracks, and facilitates the calculation of reliable results. It reveals the deformation patterns of the deformations along the structures, which are strongly related to the human activities, engineering structures, geometries, engineering geological settings and a variety of loading scenarios. For road networks, elevated roads are more stable except a few transportation stations, such as Longyang Road and Pujiang Stations. For subway networks, elevated sections with deeper pile foundations are more stable than underground sections located in shallow soft soil, and the earlier construction sections with long-term settlement and effective management are more stable than the later construction sections. For high-speed railways, the subsidence is much smaller and a subsidence A is identified. Such observations of engineering-scale deformation on linear structures can help engineers evaluate the stability of urban infrastructures in a fast and reliable way, so as to improve hazard assessment.

Several issues are still open for further improvement. There is no encompassing method for assessment of all civil infrastructures. Thus, our PSI analysis approach must optimized for each particular case. Based on the existing monitoring network, future ground subsidence

detection systems for urban infrastructures will require a close collaboration of different disciplines, including the InSAR remote sensing, geophysics, hydrogeological, civil engineering, and so on.

## 5. ACKNOWLEDGEMENTS

This work is supported by the National Natural Science Foundation of China (Grant No. 61331016), the Province Natural Science Foundation of Hubei (Grant No. 2014CFA047). Thanks for the TerraSAR-X datasets provided by DLR and Shanghai Institution of Geological Survey through the AO project (GEO0606).

## 6. REFERENCES

[1] M. Crosetto, O. Monserrat, M. Cuevas, et al. "Measuring thermal expansion using X-band Persistent Scatterer Interferometry," *Isprs J. Photogramm. Remote Sens.*, vol. 100, pp. 84-91, May 2014.

[2] X. Qin, M. Yang, H. Wang, et al. "Application of high-resolution PS-InSAR in deformation characteristics probe of urban rail transit," *Acta Geodaetica et Cartographica Sinica*, vol. 45, no. 6, pp.713-721, Jun. 2016.

[3] H. Lan, L. Li, H. Liu, et al. "Complex Urban Infrastructure Deformation Monitoring Using High Resolution PSI." *IEEE J. Sel. Topics Appl. Earth Observ. Remote Sens.*, vol. 5, no. 2, pp. 643-651, Apr. 2012.

[4] K. Dai, G. Liu, B. Yu, et al. "Detecting subsidence along a high speed railway by ultrashort baseline TCP-InSAR with High Resolution Images," *ISPRS - International Archives of the Photogrammetry*, pp. 61-65, 2013.

[5] Q. Zhao, A. Pepe, W. Gao, et al. "A DInSAR investigation of the ground settlement time evolution of ocean-reclaimed lands in Shanghai," *IEEE J. Sel. Topics Appl. Earth Observ. Remote Sens.*, vol. 8, no. 4, pp. 1763-1781, Apr. 2015.

[6] L. Chang, R. F. Hanssen. "Detection of cavity migration and sinkhole risk using radar interferometric time series". *Remote Sensing of Environment*, vol. 9, pp. 56-64, 2014.

[7] X. Shi, M. Liao, T. Wang, et al. "Expressway deformation mapping using high-resolution TerraSAR-X images". *Remote Sensing Letters*, vol. 2, pp. 194-203, 2014.

[8] A. Hooper, H. Zebker, P. Segall, and B. Kampes, "A new method for measuring deformation on volcanoes and other natural terrains using InSAR persistent scatterers," Geophys. Res. Lett., vol. 31, no. L23611, 2004.

[9] U. Wegmüller, D. Walter, V. Spreckels, et al. "Nonuniform ground motion monitoring with TerraSAR-X Persistent Scatterer Interferometry," *IEEE Trans. Geosci. Remote Sens.*, vol.48, no. 2, pp. 895-904, Feb. 2010.

[10] O. Mora, J. J. Mallorqui, A. Broquetas. "Linear and nonlinear terrain deformation maps from a reduced set of interferometric SAR images," *IEEE Trans. Geosci. Remote Sens.*, vol. 10, no. 41, pp. 2243-2253, Oct. 2003.